



Limnological, Sediment, and Aquatic Macrophyte Biomass Characteristics in Half Moon Lake, Eau Claire, Wisconsin, 2013



Interim Letter Report 1 November, 2013

William F. James
University of Wisconsin – Stout
Sustainability Sciences Institute Discovery Center – 123 E Jarvis Hall
Center for Limnological Research and Rehabilitation
Menomonie, Wisconsin 54751

BACKGROUND AND OBJECTIVES:

Management to reduce internal phosphorus (P) loading and algal growth to improve underwater light condition for native aquatic plants has been threefold for Half Moon Lake, Eau Claire, Wisconsin (James et al. 2002). Motor boat activity has been restricted on the lake to reduce P resuspension. Canopy-shading of native macrophytes and P recycling caused by curly-leaf pondweed decomposition have been controlled by annual early spring herbicide treatments during the years 2009-2013 and beyond to selectively target this species with minimal impact to native plants. Finally, P release from sediments was managed during the year 2011 (application occurred during 15-18 June, 2011) using buffered alum-aluminate to drive algal productivity toward P-limited growth. The goal was to decrease internal P loading from sediment by at least 90% in order to reduce algal biomass and increase light penetration. The objectives of this interim letter report are to describe limnological conditions and aquatic macrophyte response in 2013 to overall lake rehabilitation.

METHODS:

Lake Limnological Monitoring

Six stations were established in the lake for water quality monitoring purposes (Figure 1; Table 1). Monitoring was conducted biweekly at each station between May and October, 2013. Water temperature, dissolved oxygen, conductivity, and pH were measured in situ at 0.5-m intervals using a sonde unit (Hydrolab Quanta, Hach Inc., Loveland, CO) that was precalibrated against known standards and Winkler titrations. Secchi disk transparency was measured at each station by lowering a 20-cm diameter alternating black and white disk into the water column until it could not be seen, then slowly pulling it back up until visible, and recording the depth of visibility. Underwater photosynthetically-active radiation (PAR) was measured at 25-cm intervals using a cosine quantum radiometer (Model LI1000, Li-Cor, Inc., Lincoln, NE). The light attenuation coefficient was calculated as,

$$k_d = \frac{\ln(I_o) - \ln(I_z)}{z}$$

where I_o is the surface PAR ($\mu\text{E}/\text{cm}^2 \text{ s}$) and I_z is the PAR at depth z (m). In general, k_d is inversely related to Secchi disk transparency. Thus, higher k_d reflects lower light penetration into the water column and a lower Secchi disk transparency.

Water samples integrated over the upper 1 m were collected biweekly for analysis of total P, soluble reactive P, viable chlorophyll, and total alkalinity. Total P samples were predigested with potassium persulfate according to Ameer et al. (1993). Total and soluble reactive P (i.e., P available for uptake by algae) were analyzed colorimetrically using the ascorbic acid method (APHA 2005). Samples for viable chlorophyll (i.e., a surrogate measure of algal biomass) were filtered onto glass fiber filters (Gelman A/E; 2.0 μ nominal pore size) and extracted in 50:50 dimethyl sulfoxide:acetone before fluorometric determination (Welchmeyer 1994). Total alkalinity was determined via titration of unfiltered water samples with 0.02 N sulfuric acid to a pH endpoint of 4.8 according to APHA (2005).

Storm Sewer Monitoring

Automated storm water samplers (ISCO model 6700) and flow loggers equipped with area-velocity sensors (ISCO model 4150) were deployed at 4 storm sewers in 2013 to determine phosphorus concentration and loading (Figure 1). Loggers were programmed to monitor stage and velocity at 5- to 15-min intervals. Storm water samplers collected discrete samples at 15-min intervals during precipitation and runoff events. The discrete samples were composited via flow-weighting in the laboratory for determination of total and soluble reactive P.

Sediment Chemistry

Sediment cores were collected at station 10 and 30 in August, 2013, for determination of sediment P fractions and rates of P release under anoxic conditions. One core from each station was sectioned at 1- to 2.5-cm intervals for determination of loosely-bound, iron-bound, and aluminum-bound P using methods described in Hieltjes and Lijklema (1980), Psenner and Puckso (1988), and Nürnberg (1988). Additional subsamples were dried at 105 °C to a constant weight and burned at 500 °C for determination of moisture content, sediment density, and organic matter content (Håkanson and Jansson 2002). Five replicate cores were also collected at each station for determination of P release from sediment under anoxic conditions. The cores were drained of overlying water and the upper 10 cm of sediment was transferred intact to a smaller acrylic core liner (6.5-cm dia and 20-cm ht) using a core remover tool. Surface water collected from the lake was filtered through a glass fiber filter (Gelman A-E) and 300 mL was siphoned onto the sediment contained in the small acrylic core liner without causing sediment resuspension. Sediment incubation systems were placed in the darkened environmental chamber and incubated at a constant temperature (20 °C). The oxidation-reduction environment in the overlying water was controlled by gently bubbling nitrogen (anoxic) through an air stone placed just above the sediment surface in each system.

Water samples for soluble reactive P were collected from the center of each system using an acid-washed syringe and filtered through a 0.45 µm membrane syringe filter (Nalge). The water volume removed from each system during sampling was replaced by addition of filtered lake water preadjusted to the proper oxidation-reduction condition. These volumes were accurately measured for determination of dilution effects. Soluble reactive P was measured colorimetrically using the ascorbic acid method (APHA 2005). Rates of P release from the sediment ($\text{mg}/\text{m}^2 \text{ d}$) were calculated as the linear change in mass in the overlying water divided by time (days) and the area (m^2) of the incubation core liner. Regression analysis was used to estimate rates over the linear portion of the data.

Aquatic Macrophytes

In June and August, 2013, submersed macrophyte biomass was quantified at ~150 stations in the lake using the point-intercept method (Madsen, 1993). In late April, numbers of germinated curly-leaf pondweed turions per square meter were quantified at each station. A rake-pull method was used to collect samples. The rake was lowered to the sediment and raised to the lake surface at a constant, slow rate while twisting the handle to snag macrophyte stems within a ~ 0.13 m² area. The samples were sorted by species and dried to a constant mass at 65 °C in a forced-air drying oven. Biomass (g/m²) at each station was estimated as dry mass divided by the circular area covered by a 180 degree twist of the rake. The rake-pull method provides a reasonably accurate biomass estimate for species such as curly-leaf pondweed and Eurasian watermilfoil that is comparable to diver quadrat sampling (Johnson 2010). However, it overestimates biomass in areas dominated by coontail, elodea, and flat-stemmed pondweed because these species tend to inter-tangle with plants outside the quadrat area, resulting in unintended sampling from an area wider than that of the rake diameter (Johnson 2010). Thus, caution needs to be used when interpreting biomass data dominated by these species.

RESULTS:

Sediment characteristics in 2013

Al treatment occurred during the period 15-18 June, 2011. The target dosage goal for the western arm of the lake was 150 g Al/m² while the eastern arm and southern (i.e., south of the causeway) embayment target concentration was 75 g Al/m². Braun's Bay was not treated with Al.

Aluminum hydroxide was clearly visible in the upper 3-4 cm sediment layer as a white precipitate in many of the collected cores (Figure 2). Al treatment was very effective in binding loosely-bound and iron-bound P (i.e., the fraction most active in

diffusive P flux) in the upper sediment layer in both arms after two years post-treatment (Figure 3). Concentrations of iron-bound P in 2013 were near zero in the upper 3-cm sediment layer at both stations, suggesting binding of nearly this entire fraction onto the Al floc. In contrast, iron-bound P concentrations in the upper 1-cm sediment layer approached 2 mg/g at station 10 and 0.4 mg/g at station 30 in 2010, one year before Al treatment (Figure 3). Rates of P release from sediment under anoxic conditions (Figure 4) were zero in 2013 versus rates that exceeded 8 mg/m² d in 2010 (data not shown).

Water quality trends after Al treatment

Total P concentrations exhibited a peak at all stations in late May (Figure 5) that was probably associated with high zooplankton biomass (versus algal biomass). Chlorophyll concentrations peaked two weeks before the total P maximum in late May then generally declined during the total P peak (Figure 6). Secchi transparency increased to a maximum in late May in conjunction with lower chlorophyll concentrations (Figure 7) and k_d (i.e., attenuation of photosynthetically active radiation) was less than 1 m⁻¹ (Figure 8). These patterns were consistent with the suggestion that zooplankton grazing was high, resulting in a late spring clearing phase.

In the deeper western arm of the main basin (i.e., stations 10 and 20), chlorophyll concentrations and k_d were relatively low, while Secchi transparency was high through mid-July (Figure 6-8). In particular, chlorophyll concentrations were low at 10-20 µg/L and PAR penetration reached the lake bottom during this period. Total P and chlorophyll concentrations increased in the western arm between late July and the end of September, coinciding with declines in Secchi transparency and elevated k_d . Overall, peak and mean chlorophyll concentrations in July through September were modest at ~ 35 µg/L and 25 µg/L, respectively, while mean Secchi transparency was 1.5 m during this late summer period. Total P concentrations increased in the western arm in conjunction with elevated chlorophyll, indicating some P assimilation by algae, and the mean July-September concentration was 39 µg/L.

The eastern arm (stations 30 and 40) and south embayment (station 50) areas of the lake exhibited seasonally lower total P, chlorophyll, and k_d , and high Secchi transparency, during the height of the phytoplankton growing season compared to the western arm (Figures 5-8). In particular, July-September mean total P concentrations were only $\sim 26 \mu\text{g/L}$ in association with very low mean chlorophyll at $\sim 13 \mu\text{g/L}$ and Secchi disk transparency that extended to the lake bottom (i.e., $\sim 2 \text{ m}$).

Trends at station 60 (i.e., Braun's Bay) were also much improved in 2013 versus 2012. Although total P concentrations fluctuated and exhibited peaks near or in excess of $40 \mu\text{g/L}$ in late May early July, and late September (Figure 5), chlorophyll concentrations were very low (Figure 6) and Secchi disk transparency extended to the lake bottom (Figure 7) throughout the summer. These patterns suggested that total P peaks were perhaps the result of high zooplankton biomass versus incorporated into algal biomass. The PAR attenuation coefficient was low and varied between ~ 1.4 and 0.8 m^{-1} (Figure 8), indicating good solar radiation penetration down to the lake bottom for submersed aquatic macrophyte growth.

Hypoxic and anoxic (i.e., D.O. $< 2 \text{ mg/L}$) conditions rarely occurred above the sediment interface during the study period the summer (Figure 9). Hypoxia was evident in June and July at station 60 and in August at stations 30 and 50. In contrast, concentrations were well above 2 mg/L throughout the summer at station 40 and stations located in the western arm (station 10 and 20). Relatively high dissolved oxygen near the lake bottom most likely coincided photosynthetic production by submersed aquatic macrophyte growth (primarily elodea).

Overall trends in July-September mean total P, chlorophyll, and Secchi disk transparency in the main basin (i.e., stations 10-40) are shown in Figure 10. The period July-September was chosen because it represented the typical period of maximum nuisance algal blooms and did not include the late May-June clearing phase caused by zooplankton grazing. Mean total P and chlorophyll in the main basin of the lake (i.e., stations 10 – 40) remained low, while Secchi transparency was high, in 2013 relative to

pre-AI treatment years; means were also comparable to those for 2011 and 2012. Overall, mean AI post-treatment total P and chlorophyll declined to ~ 30 and 21 $\mu\text{g/L}$, respectively, representing a greater than 60% decrease over pretreatment values. The mean post-AI treatment Secchi transparency of 1.65 m represented a 2X increase in water clarity over the pretreatment mean. Predicted maximum inhabitable depth for stem- and rosette-forming submersed macrophytes, based on the percentage of surface PAR radiation penetrating the water column (Middelboe and Markager 1997), remained improved in 2013 over pre-AI treatment (Figure 11). Underwater light habitat improvement was greatest for stem-forming submersed macrophytes, suggesting that nearly the entire lake bottom was favorable for growth in 2013. Maximum inhabitable depth for rosette-forming submersed macrophytes remained greater than 1 m after AI treatment. This predicted depth was lower than for stem-forming submersed macrophytes due to the compact growth patterns of rosette-forming species in relation to the river channel morphometry of Half Moon Lake (i.e., relatively steep sides with a deeper expansive thalweg). As of 2013, the maximum colonizable depth essentially doubled in conjunction with AI treatment.

There was also a strong linear relationship between mean total P and chlorophyll for all sampling years, suggesting that P played an overall important role in both limiting and stimulating algal growth (Figure 12). In both the main (i.e., the eastern and western arms; stations 10-40) and southern (i.e., south of the causeway; station 50) basin of the lake, mean concentrations of total P and chlorophyll continued to be much lower in 2013 compared to pre-AI treatment means. Mean Secchi disk transparency was higher in both regions of the lake in 2013 versus pre-alum treatment years, and inversely related to mean chlorophyll and total P (Figures 13 and 14), indicating that interrelationships between algal biomass and assimilated P were regulating water clarity in the lake.

During the July-September period of 2013, mean total P and chlorophyll concentrations were greatest in the West arm of the lake at 0.039 mg/L and 24.8 $\mu\text{g/L}$, respectively (Figure 15). The East arm and South Bay means were lower; mean total P was less than 0.030 mg/L and mean chlorophyll was less than 15 $\mu\text{g/L}$. Mean Secchi disk

transparency essentially extended to the lake bottom during the July-September time period in the East arm and South Bay versus a mean of ~ 1.5 m in the West arm. Mean k_d was very good at all locations at $\sim 1 \text{ m}^{-1}$.

Post herbicide treatment trends in curly-leaf pondweed and native submersed vegetation

2013 represented the fifth consecutive year of Endothall treatment to reduce the curly-leaf pondweed turion bank in the sediment. As of April, 2013, before the early May, 2013, herbicide treatment (i.e., after 4 consecutive early spring herbicide treatments; 2009-2012), germinated curly-leaf pondweed turions were present at only 32% of the 150 sampling sites versus a pretreatment frequency of $\sim 80\%$ in 2009 (Figure 16). In addition, the lake-wide mean density has declined to only 5 germinated turions/ m^2 in 2013 compared to the pre-treatment mean of ~ 40 germinated turions/ m^2 . Overall, both frequency and numbers of germinated turions/ m^2 declined linearly between 2010 and 2012 and has leveled off in 2013. Germinated turion frequency and density will be determined in April, 2014, to evaluate conditions after 5 years of herbicide management.

The consecutive Endothall treatments continued to be very effective in controlling early summer cohorts of curly-leaf pondweed (Figure 17). In June, 2013, curly-leaf pondweed was not detected at any sampling sites (Figure 17). However, mature curly-leaf pondweed was detected in the main basin directly west of station 30 and in shallow areas along the western shoreline of the east arm by August, 2013. Current locations and frequencies of curly-leaf pondweed during the summer, 2013, will be provided from the more detailed survey conducted by the Wisconsin DNR.

Native submersed macrophyte biomass was again dominated by Elodea in 2013, although some other native species were also observed (Stargrass, wild celery, coontail). Native biomass was relatively low in June, 2013, compared to June, 2011 and 2012 (Figure 18). This pattern was probably related to the severe wind shear in late May, 2012, that uprooted a substantial portion of the community and impacted growth. However, occurrence and biomass in August, 2013 exceeded pre-treatment levels, suggesting that

the native macrophyte community was rebounding from the stress imposed by the wind shear. Interannual trends continued to suggest that native macrophyte biomass (primarily as *Elodea*) has been increasing and recovering to pre-treatment levels since initiation of herbicide treatments in 2009. However, native dominance shifted from coontail to *Elodea* as a probable result of the 2,4-D application in 2009 to control Eurasian watermilfoil (EWM). EWM has not been observed since 2009.

Storm sewer hydrology and phosphorus inputs to Half Moon Lake

During the summer period, monthly rainfall was above normal in May and June, 2013, but substantially below normal in July through September, 2013 (Figure 19). Storm frequency and intensity were also greatest in May through mid-June, 2013, with greater than 1 inch of rainfall occurring on several occasions (Figure 20). Although numerous small storms less than 0.5 inches occurred between July and September, 2013, conditions were generally very dry with minor watershed runoff.

Overall, ~ 50 storm-related flow events were collectively captured at storm sewers 1, 2, 3, and 4 for determination of total and soluble reactive P concentrations in 2013 (Figures 21-24). In addition, 13 base flow samples were collected at storm sewer 1 between February and October. Flow increased at all monitored storm sewers as a result of storms (Figures 21-24). Storm sewers 1 and 3 drained larger watershed areas and exhibited higher flow peaks versus storm sewers 2 and 4.

At storm sewer 1, shallow groundwater pumps (up to 3 pumps) provided a continuous base flow of Chippewa River groundwater to Half Moon Lake to maintain pool elevation. Three pumps were operational between mid-June and September, providing a base flow of ~ 3.0 ft³/s (Figure 21).

Mean summer (i.e., June-September) storm flows were only slightly higher at storm sewer 3 and 4 in 2013 compared to other years (Figure 25 and Table 2). Mean summer storm flows in 2013 were similar to other years for Sewers 1 and 2. Mean base flow at

storm sewer 1 was much greater in 2013 versus other years because all pumps were operational during much of the summer. In 2013, mean storm flow was greatest at sewer 1 and 3, at 0.157 and 0.219 ft³/s, followed by sewer 2 at 0.020 ft³/s. Mean storm flow was lowest for sewer 4 at only 0.007 ft³/s.

Overall, mean storm flow-weighted total P concentrations were greatest for storm sewer 1 in 2013 at 0.417 mg/L (Figure 26 and Table 3). However, this 2013 mean was comparable to the mean concentration at this station during other years (Figure 26 and Table 3). Base-flow total P at sewer 1 was also high at 0.108 mg/L and comparable to base-flow concentrations during other years. At the other sewers, mean total P was moderately high at 0.098 and 0.204 mg/L for 2 and 3, respectively, in 2013. However, these mean concentrations were substantially lower compared to 1999. Although storm flow was generally low, the mean total P concentration for sewer 4 was moderately high at 0.178 mg/L. Mean storm-related soluble reactive P concentrations were near 0.03 mg/L or below in 2013 (Figure 26 and Table 3). However, the base flow mean soluble reactive P concentration was much higher for sewer 1 in 2013 at ~ 0.043 mg/L, compared to a mean concentration of 0.01 mg/L in 1999.

Storm sewer 1 dominated total and soluble reactive P loading in 2013 (Figure 27; Tables 4 and 5). In particular, base flow P loading increased by greater than 2-fold at this sewer due to operation of three pumps in 2013. Thus, the P loading increase at this station was the result of increased base flow in 2013. Storm sewer 3, which also drains a relatively large urban watershed area, was the second greatest P contributor. P loading was minor for storm sewers 2 and 4 by comparison.

DISCUSSION AND CONCLUSIONS:

Base flow soluble reactive P loading from storm sewer 1 continued to be relatively high in 2013 versus 1999. This pattern was the result of much higher soluble reactive P concentrations in the base flow in 2013 coupled with higher base flow due to operation of three pumps versus very low concentrations and lower base flow rates in the 1999 study.

Similar to 2012, the south embayment exhibited relatively low mean total P (July-September mean = 0.026 mg/L) and chlorophyll (July-September mean = 12.6 ug/L) despite its proximity to storm sewer 1 P inflows. Short-circuiting directly to the Becca Brook outlet, located south of the storm sewer, would explain the lack of impact on the south embayment and a dye tracking study will be conducted in 2014 to better understand flow patterns in the embayment. Rhodamine WT fluorescent dye will be injected into the storm sewer and monitored as it flows into the south embayment. Dye concentration time series will be quantified at Becca Brook and the causeway bridge to determine the predominant direction of flow. This information will be used to estimate the time of travel and the residence time of the dye cloud in the lake.

Lake water quality conditions were tremendously improved in 2013, three summer's post-Al treatment. Mean July-September total P of 0.033 mg/L in the main basin was 61% lower than the pretreatment mean. The mean July-September main basin chlorophyll concentration of 19.6 µg/L represented a nearly 70% reduction over the pretreatment mean of 63 µg/L. Mean Secchi transparency in the main basin has doubled to 1.72 m since Al treatment. The improved underwater PAR has translated to a potential inhabitable depth of ~ 2.9 and 1.3 m for native stem- and rosette-forming submersed aquatic macrophytes, respectively. Numbers of germinated curly-leaf pondweed turions in April continued to decline after the fourth year of Endothall treatment. Although the wind storm of 2012 had a major impact on the aquatic macrophyte community, native submersed macrophyte biomass, dominated by Elodea, appears to have rebounded to high levels in August, 2013.

REFERENCES:

Ameel, J.J., Axler, R.P., and Owen, C.J. 1993. Persulfate digestion for determination of total nitrogen and phosphorus in low nutrient water. American Environmental Laboratory (October, 1993):8-10.

American Public Health Association. 2005. Standard methods for the examination of water and wastewater. 21th ed., Washington, DC.

Carlson, R.E. 1977. A trophic state index for lakes. *Limnol. Oceanogr.* 22:361-369.

Johnson, J.A. 2010. Evaluation of lake-wide, early-season herbicide treatments for controlling invasive curlyleaf pondweed (*Potamogeton crispus*) in Minnesota Lakes. Master's thesis, University of Minnesota.

Madsen, J.D. 1993. Biomass techniques for monitoring and assessing control of aquatic vegetation. *Lake Reserv. Manage.* 7:141-154.

Middelboe, A.L., and Markager, S. 1997. Depth limits and minimum light requirements of freshwater macrophytes. *Freshwat. Biol.* 37:553-568.

Welschmeyer, N.A. 1994. Fluorometric analysis of chlorophyll a in the presence of chlorophyll b and pheopigments. *Limnol. Oceanogr.* 39:1985-1992.

Table 1. Typical water column depths at the various water sampling stations in Half Moon Lake, Wisconsin.

Station	Nominal Depth	
	(m)	(ft)
10	3.0	9.8
20	3.0	9.8
30	2.5	8.2
40	2.5	8.2
50	2.2	7.2
60	1.8	5.9

Table 2. Comparison of mean summer flow in 1999 versus 2012-13 for various storm sewers draining into Half Moon Lake.

Sewer	Location		1999			2012			2013		
			Precip	Flow		Precip	Flow		Precip	Flow	
			(inches)	(ft ³ /s)	(m ³ /s)	(inches)	(ft ³ /s)	(m ³ /s)	(inches)	(ft ³ /s)	(m ³ /s)
1	Owen Park Pumps	Total	9.6	1.220	0.0346	8.3	1.242	0.0352	9.3	2.898	0.0821
		Storm Flow		0.048	0.0014		0.182	0.0052		0.157	0.0044
		Base Flow		1.172	0.0332		1.058	0.0300		2.742	0.0777
2	Near Middlefort Clinic		0.091	0.0026		0.022	0.0006		0.020	0.0006	
3	West of Beach		0.038	0.0011		0.046	0.0013		0.219	0.0062	
4	Carson Park					0.003	0.0001		0.007	0.0002	

Table 3. Summer flow-weighted total phosphorus (P) and soluble reactive P (SRP) for various storm sewers in 1999 and 2012-13.

Sewer	Description	1999		2012		2013	
		Total P (mg/L)	SRP	Total P (mg/L)	SRP	Total P (mg/L)	SRP
1	Storm Flow	0.344	0.038	0.358	0.019	0.417	0.015
1	Base Flow	0.074	0.010	0.109	0.040	0.108	0.043
2	Storm Flow	0.149	0.044	0.096	0.011	0.098	0.022
3	Storm Flow	0.301	0.045	0.205	0.022	0.204	0.015
4	Storm Flow					0.178	0.031

Table 4. Mean summer (JUN-SEP) total phosphorus (P) and soluble reactive P (SRP) loading for various storm sewers in 1999 and 2012-13.

Sewer	Description	1999		2012		2013	
		Total P (kg/d)	SRP	Total P (kg/d)	SRP	Total P (kg/d)	SRP
1	Storm Flow	0.042	0.005	0.161	0.009	0.285	0.010
1	Base Flow	0.211	0.029	0.283	0.104	0.644	0.256
2	Storm Flow	0.033	0.010	0.005	0.001	0.005	0.001
3	Storm Flow	0.029	0.004	0.023	0.002	0.109	0.008
4	Storm Flow					0.003	0.001

Table 5. Summer (JUN-SEP) mass loading of total phosphorus (P) and soluble reactive P (SRP) for various storm sewers in 1999 and 2012-13.

Sewer	Description	1999		2012		2013	
		Total P (kg/summer)	SRP	Total P (kg/summer)	SRP	Total P (kg/summer)	SRP
1	Storm Flow	5.03	0.56	19.46	1.03	34.44	1.24
1	Base Flow	25.53	3.45	34.19	12.55	77.91	31.02
2	Storm Flow	4.05	1.20	0.60	0.07	0.61	0.14
3	Storm Flow	3.46	0.52	2.79	0.30	13.22	0.97
						0.37	0.06

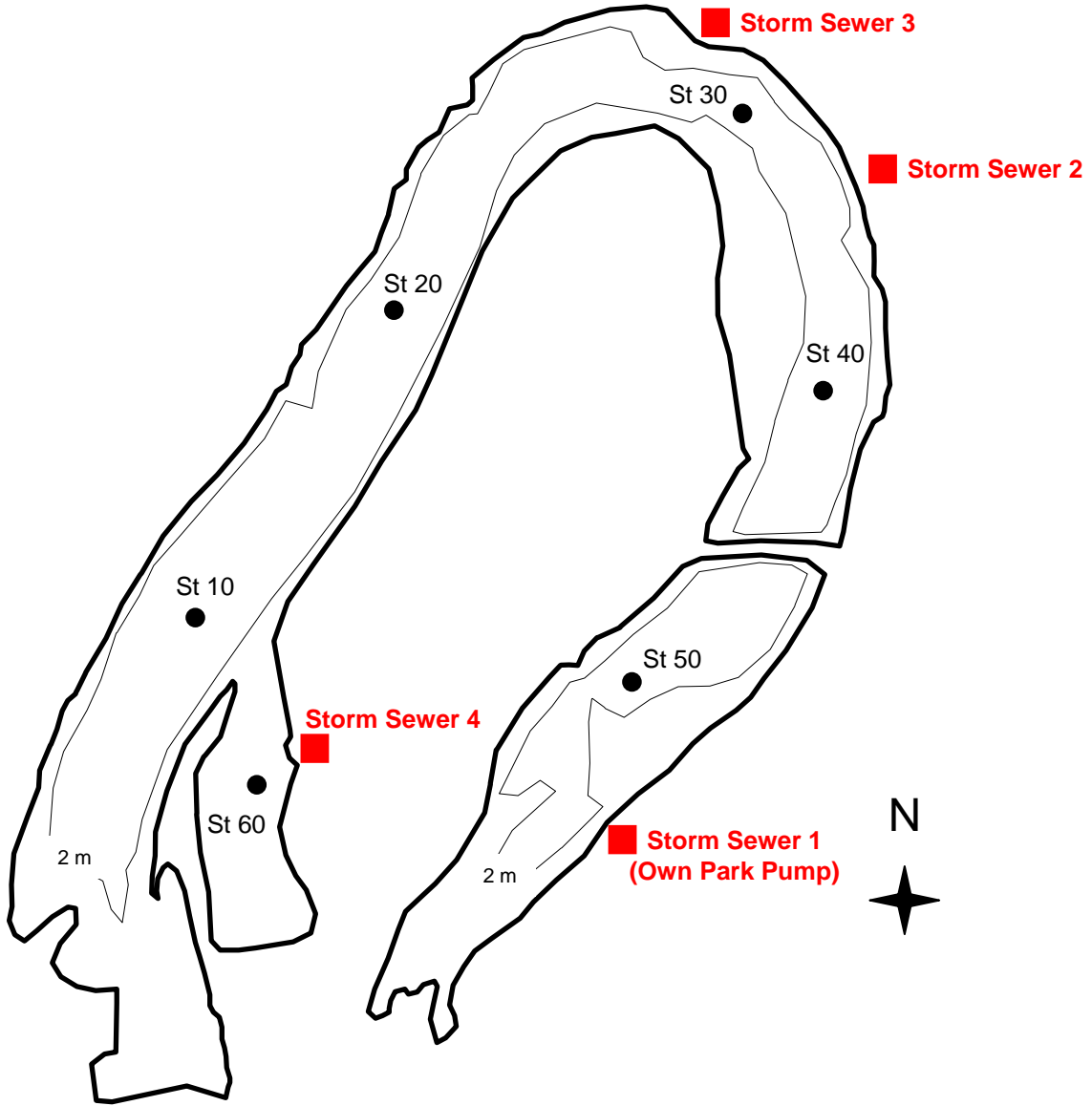


Figure 1. Sampling station locations in Half Moon Lake.

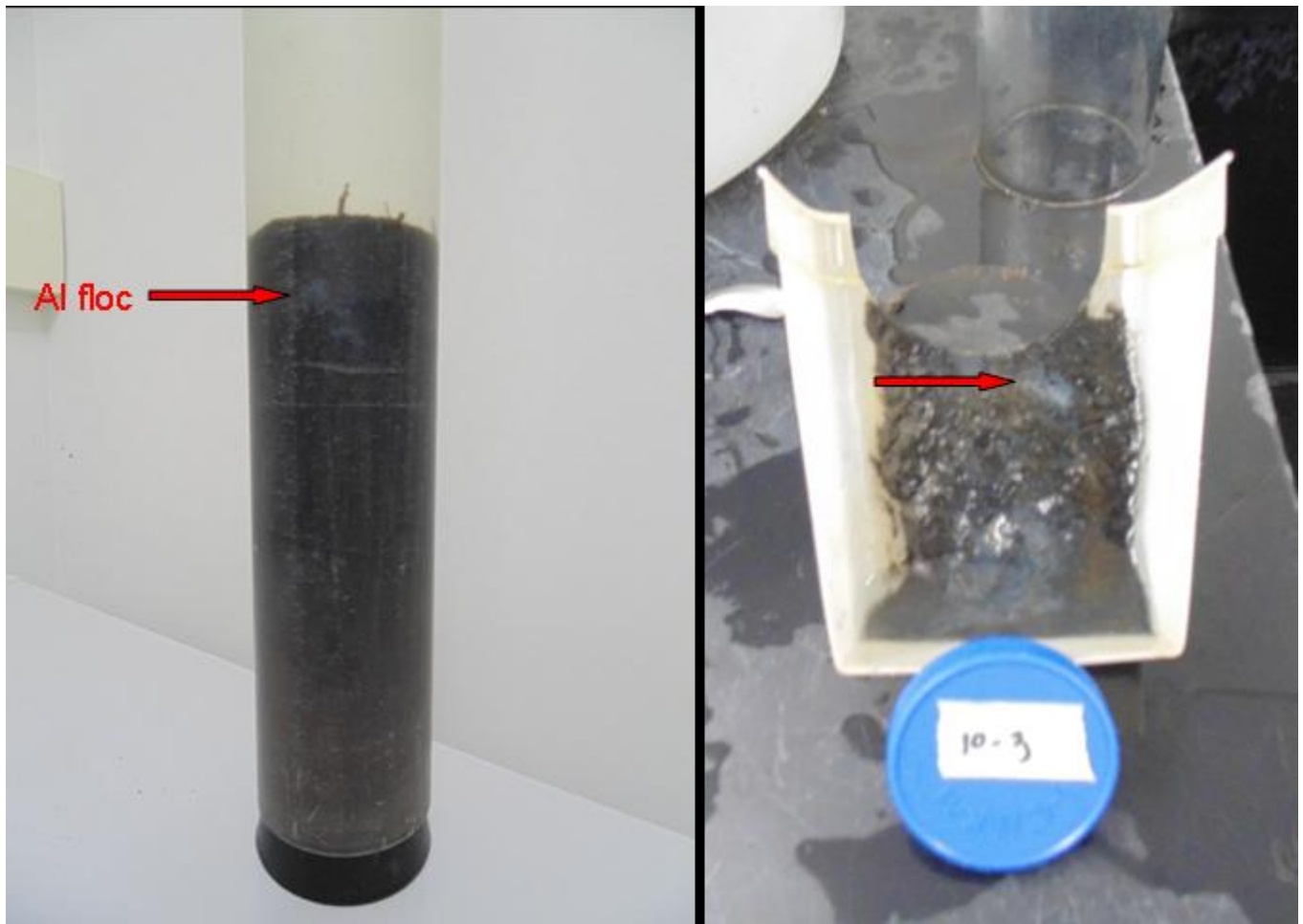


Figure 2. Al floc (white precipitate) observed in an intact sediment core (left) and in the 2-3 cm sediment core section at station 10.

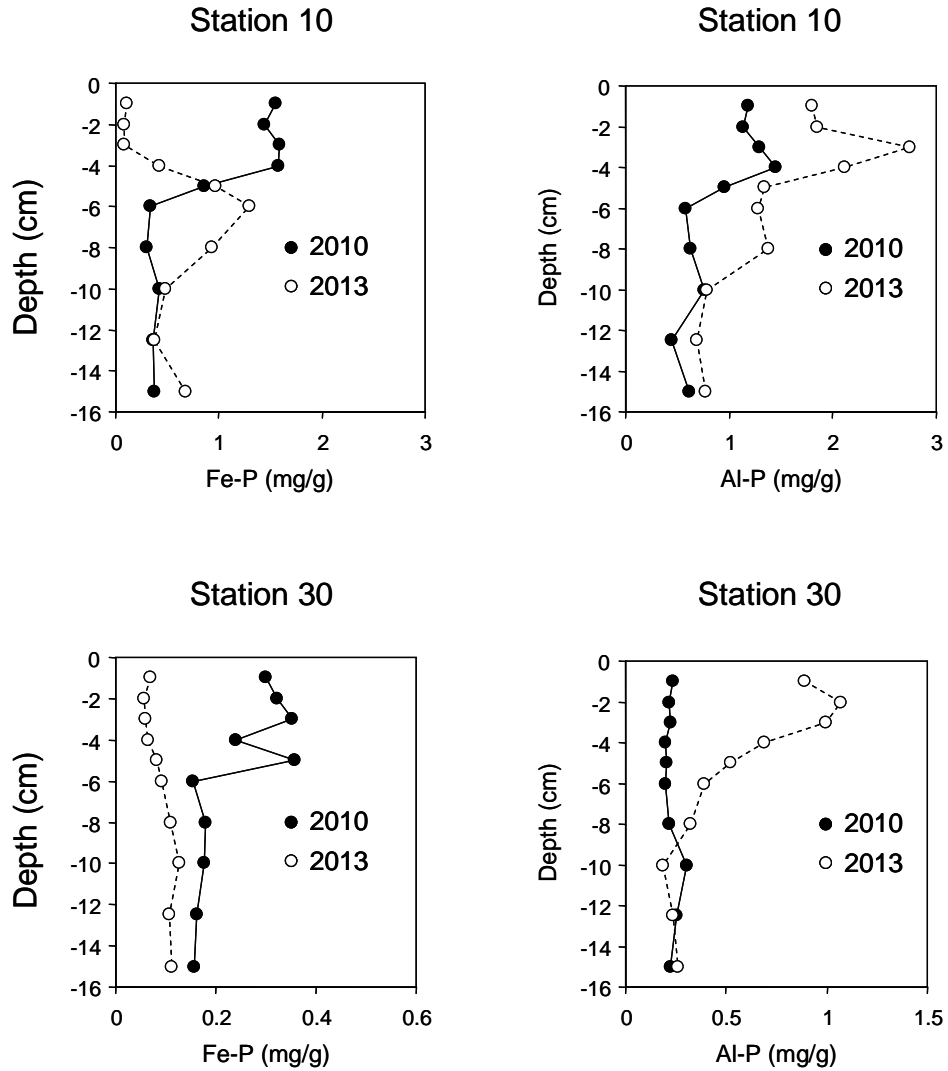


Figure 3. Variations in sediment iron-bound phosphorus (Fe-P) as a function of depth below the sediment-water interface. The year 2010 represents concentrations before alum treatment and the year 2013 represents conditions in July, two years after Al application.

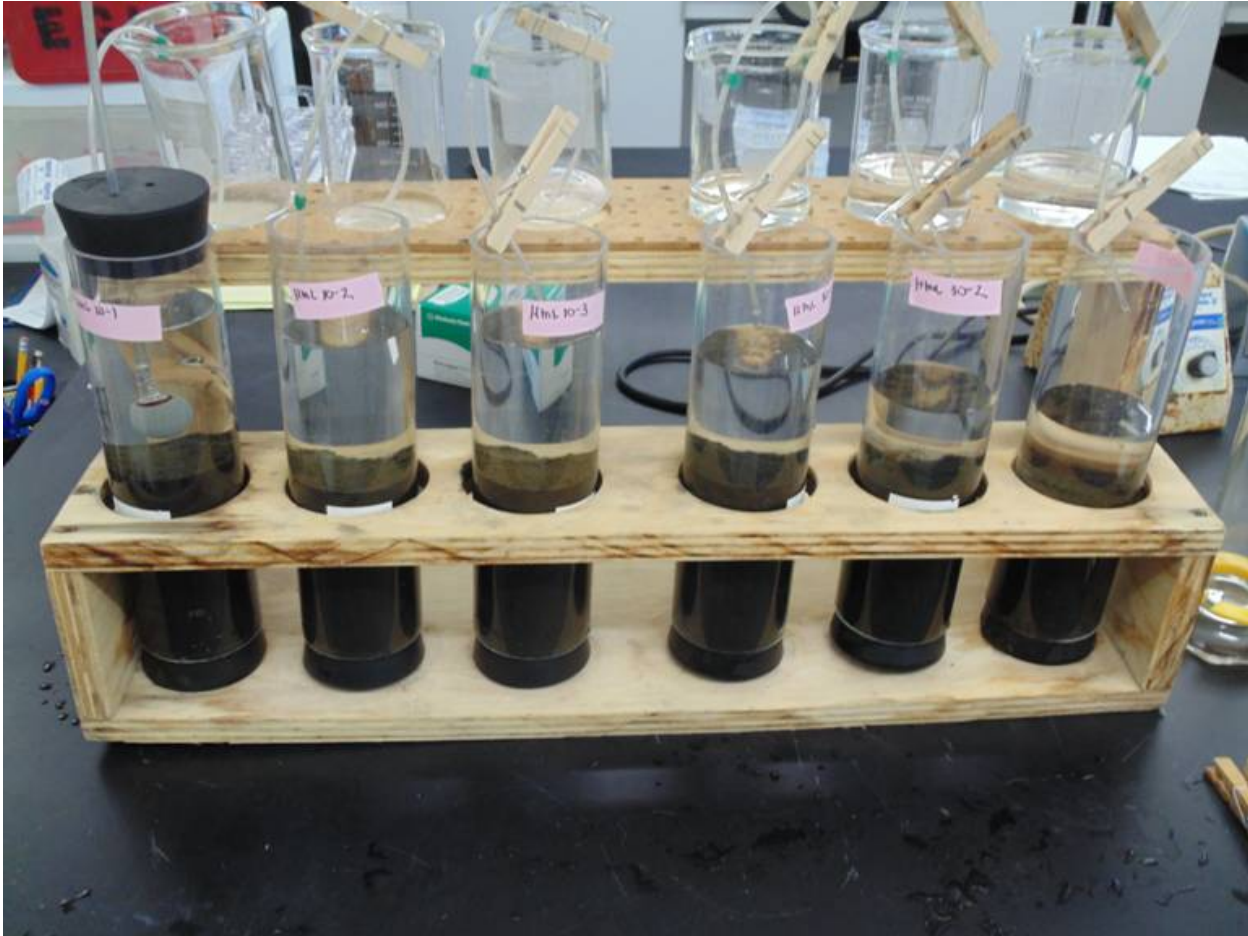


Figure 4. *Intact sediment cores being prepared for incubation under anaerobic conditions to measure rates of diffusive phosphorus flux.*

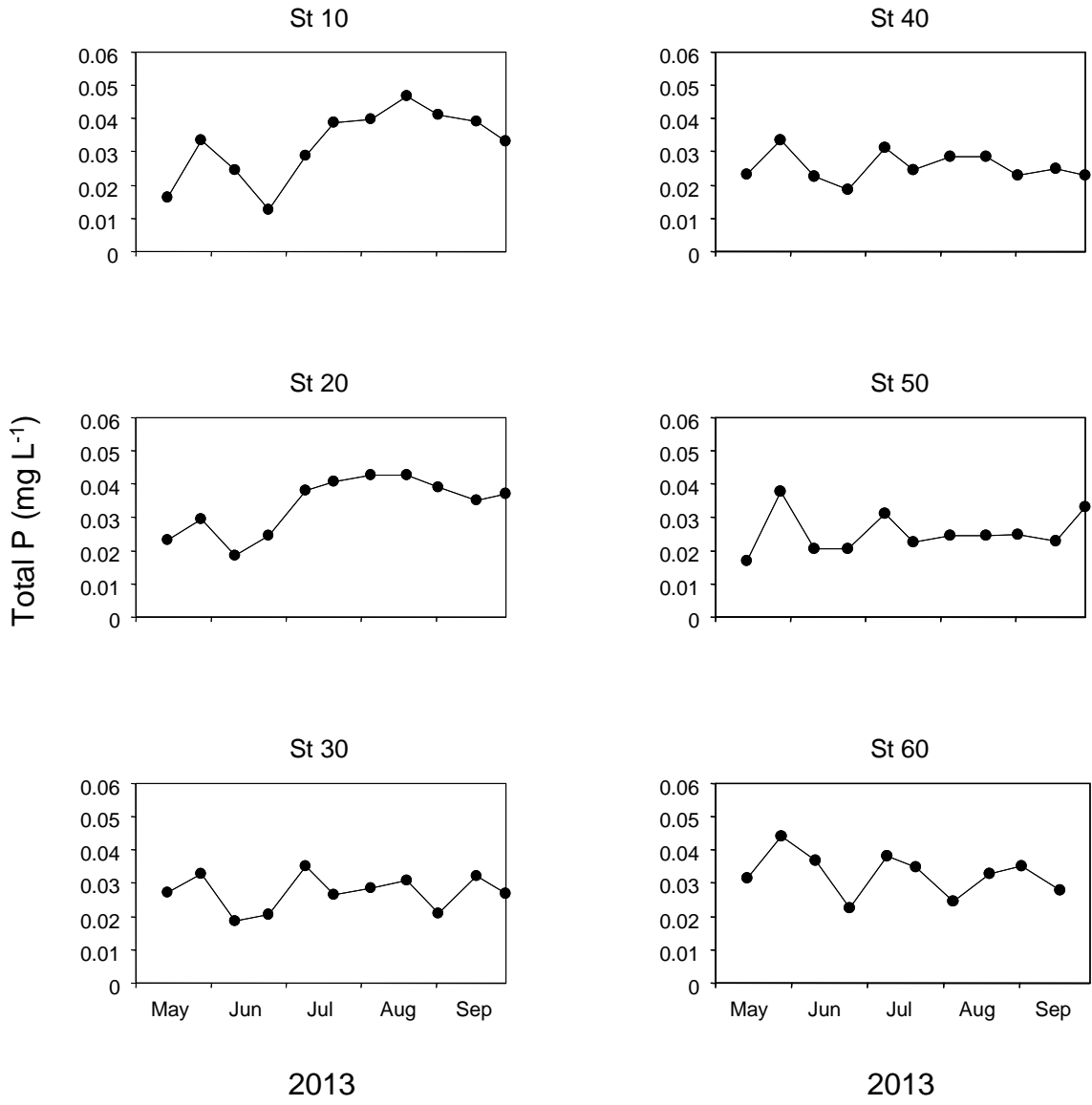


Figure 5. Seasonal variations in total phosphorus (P) at various stations in Half Moon Lake in 2013.

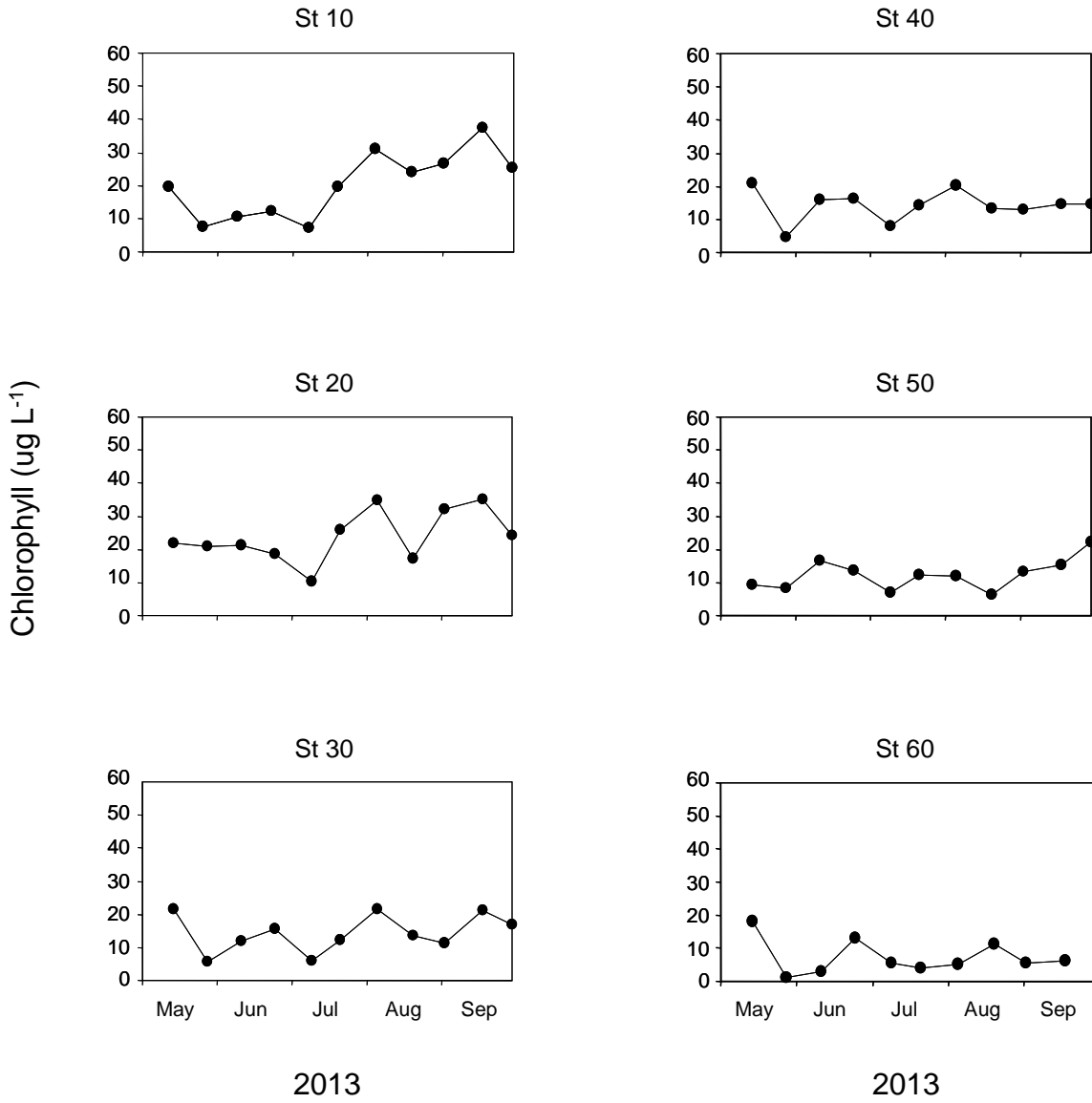


Figure 6. Seasonal variations in chlorophyll at various stations in Half Moon Lake in 2013.

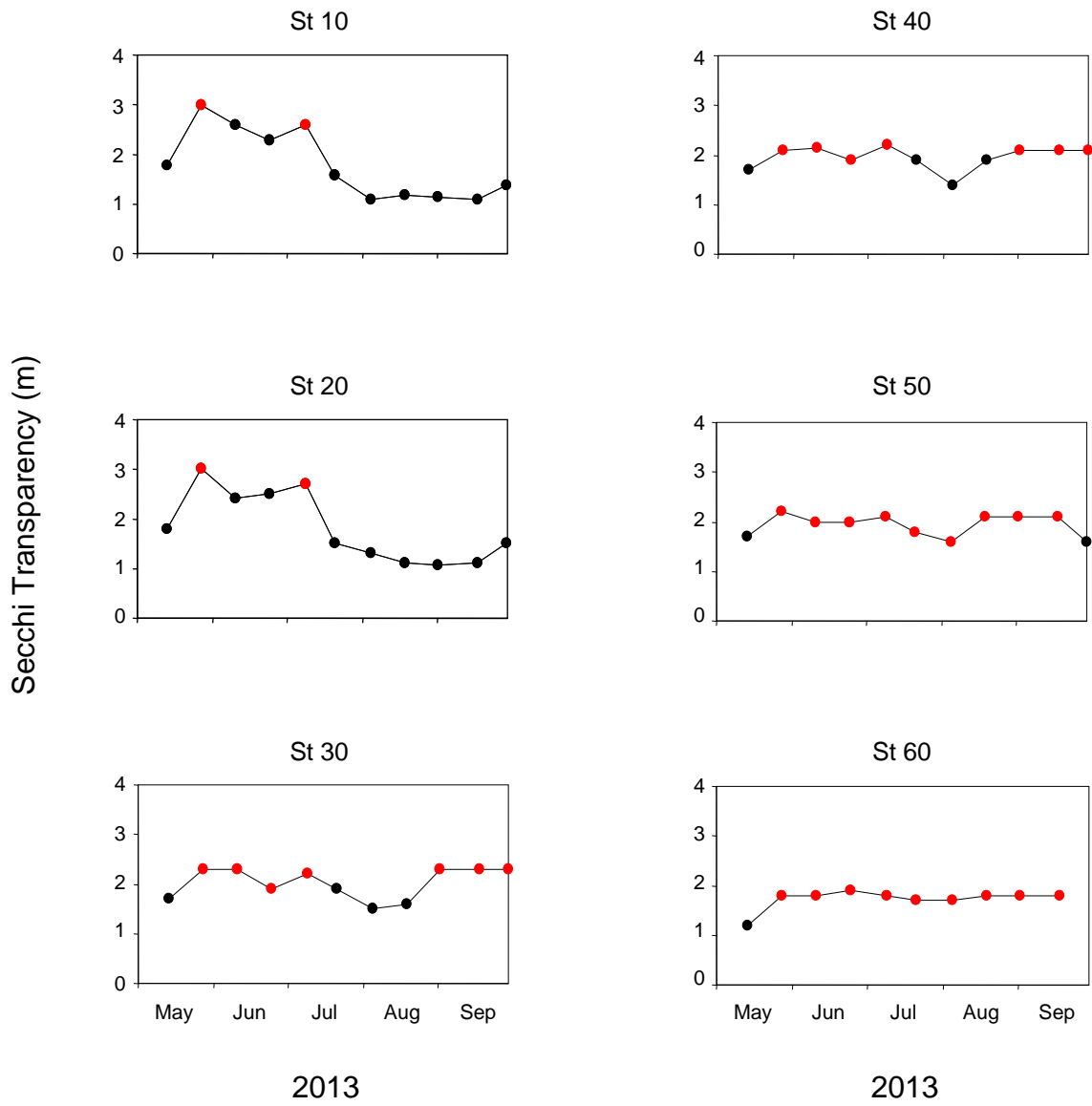


Figure 7. Seasonal variations in Secchi disk transparency at various stations in Half Moon Lake in 2013. Red circles denote periods when Secchi disk transparency was equivalent to the lake bottom depth.

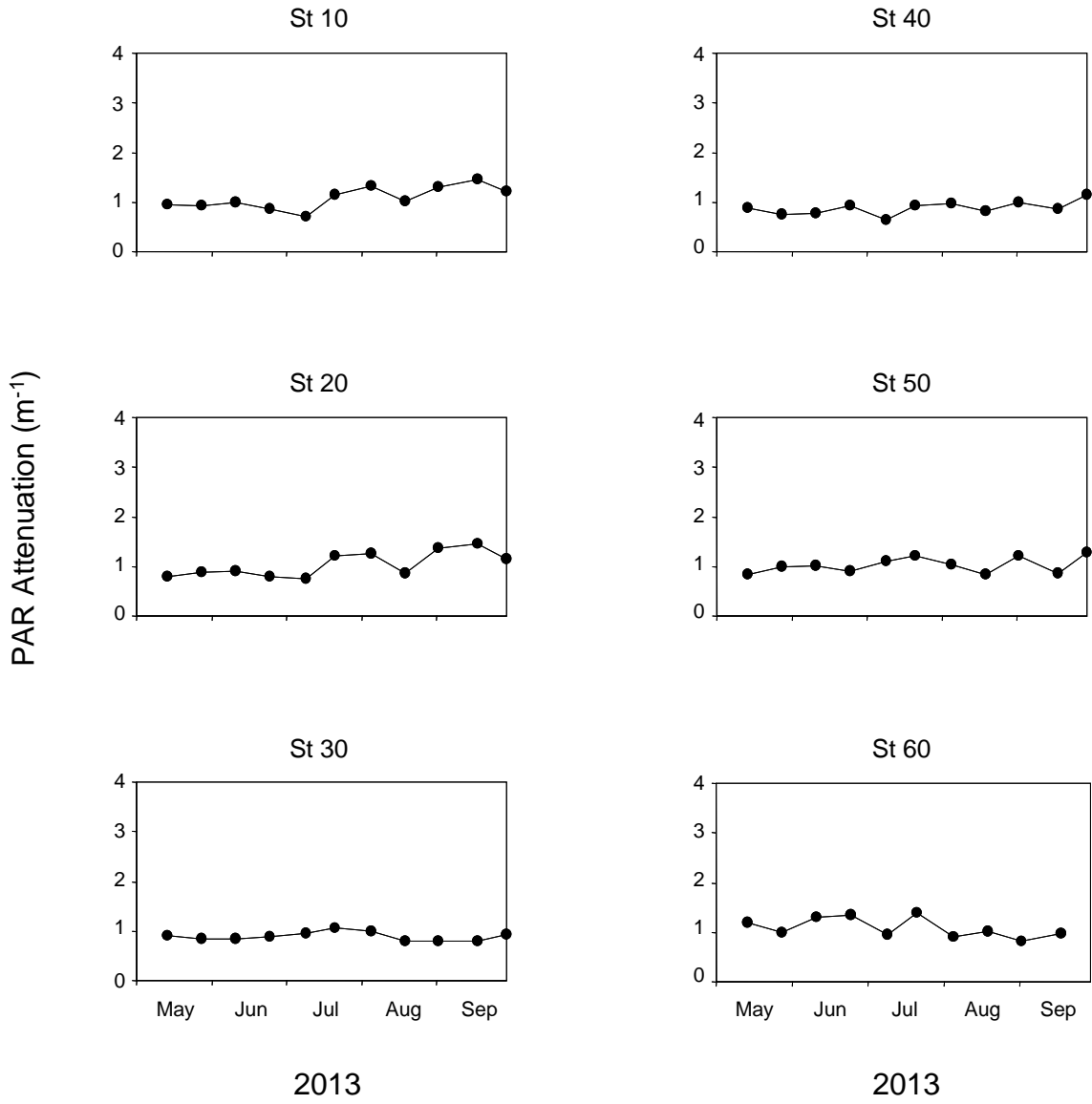


Figure 8. Seasonal variations photosynthetically active radiation (PAR) at various stations in Half Moon Lake in 2013.

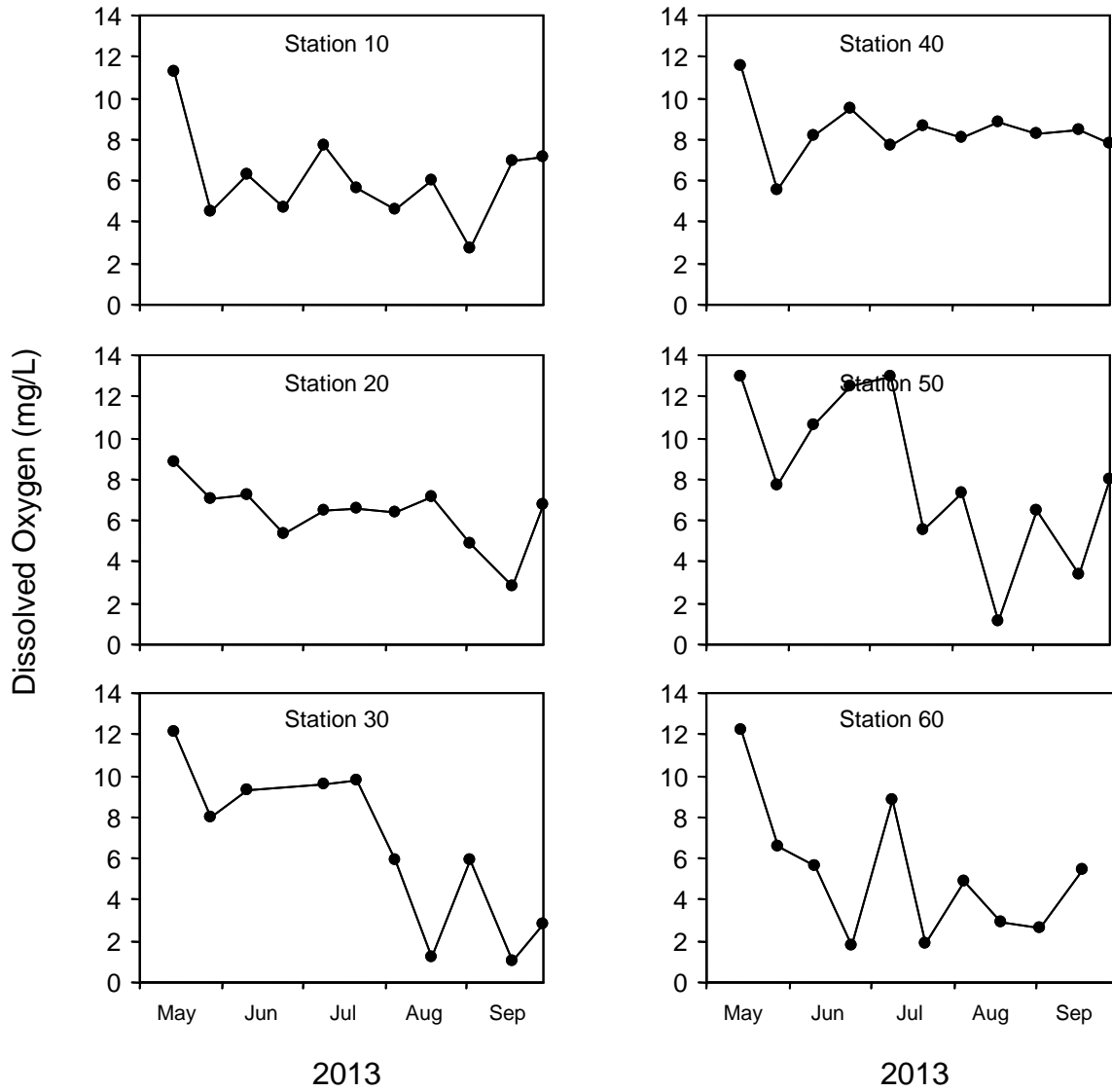
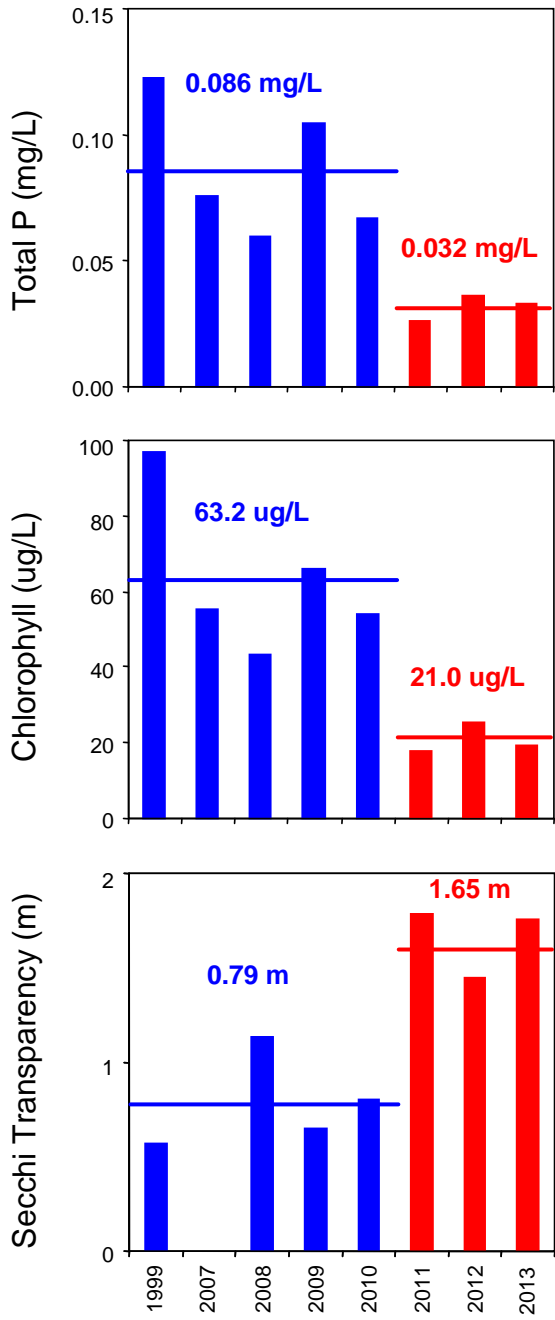


Figure 9. Seasonal variations in bottom (i.e., ~ 0.25 m above the sediment) dissolved oxygen concentration at various stations in Half Moon Lake in 2013.



Main Arm Trends JUL-SEP

(does not include Braun's Bay and the south embayment)

Figure 10. Summer (JUL-SEP) mean total phosphorus (P), chlorophyll, and Secchi transparency before (blue bars) and after (red bars) Al treatment (June, 2011). Horizontal lines represent overall pre- and post-treatment means.

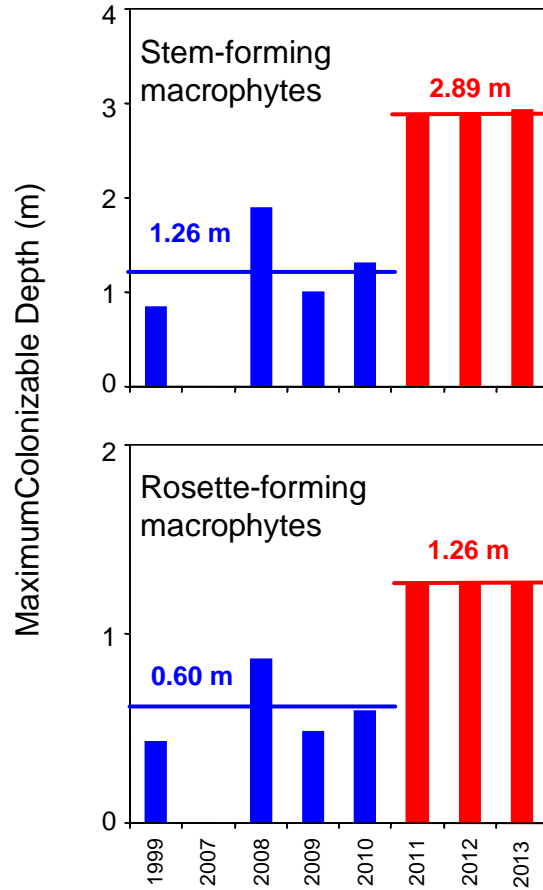


Figure 11. Summer (JUL-SEP) mean maximum inhabitable depth for stem- and rosette-forming submersed aquatic macrophytes based on Middelboe and Markager (1997) before (blue bars) and after (red bars) Al treatment (June, 2011). Horizontal lines represent overall pre- and post-treatment means.

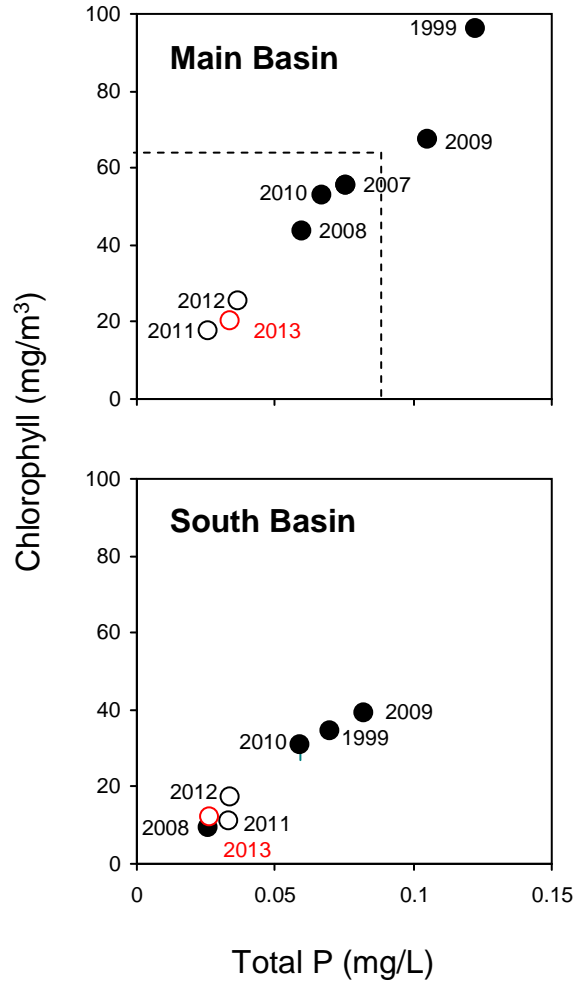


Figure 12. Summer (JUL-SEP) mean total phosphorus (P) versus chlorophyll relationships for the main (i.e., stations 10-40) and south embayment (i.e., station 50) basins. Dotted lines represent pre- Al treatment means.

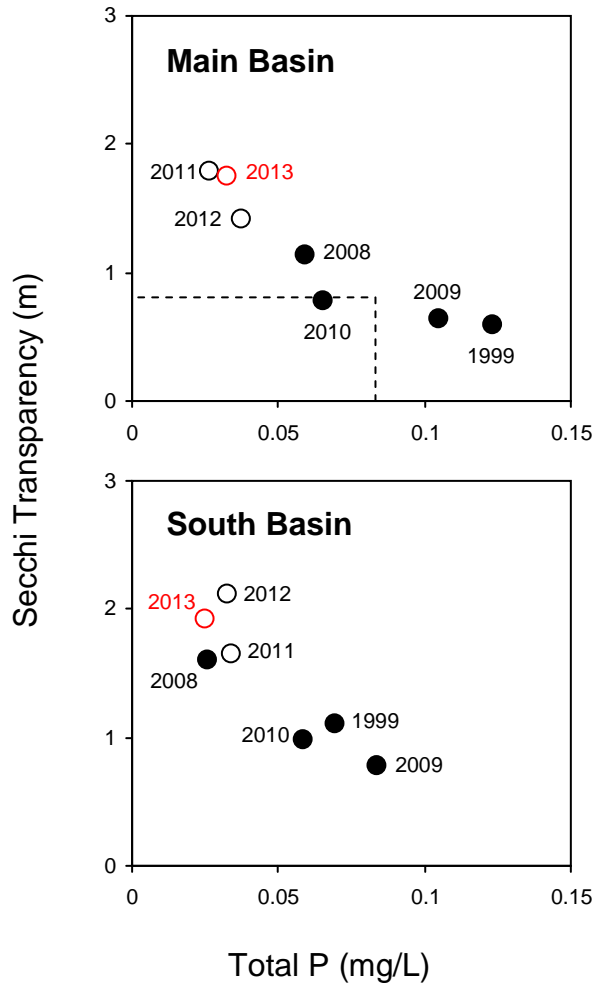


Figure 13. Summer (JUL-SEP) mean total phosphorus (P) versus Secchi transparency relationships for the main (i.e., stations 10-40) and south embayment (i.e., station 50) basins. Dotted lines represent pre- Al treatment means.

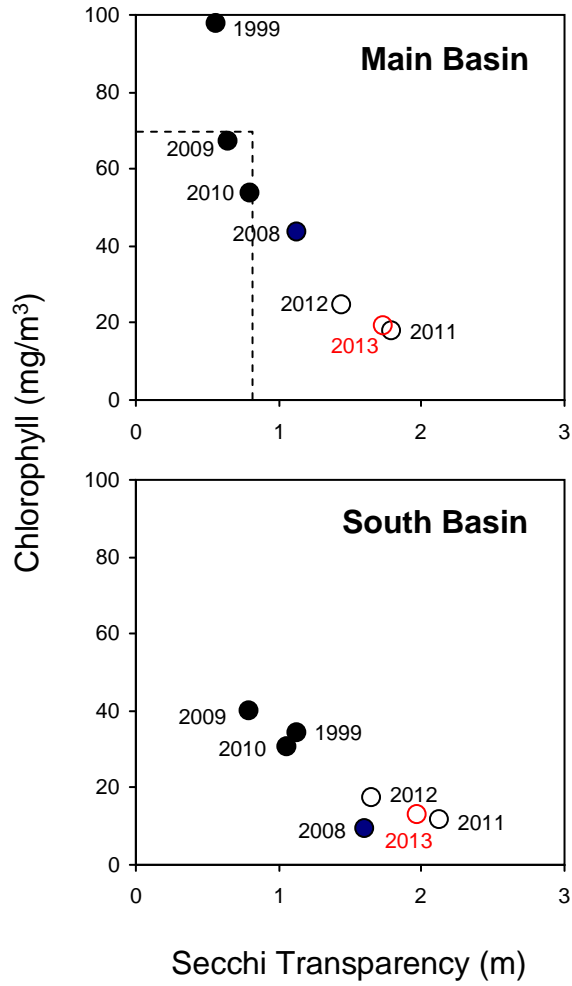


Figure 14. Summer (JUL-SEP) mean Secchi transparency versus chlorophyll relationships for the main (i.e., stations 10-40) and south embayment (i.e., station 50) basins. Dotted lines represent pre- Al treatment means.

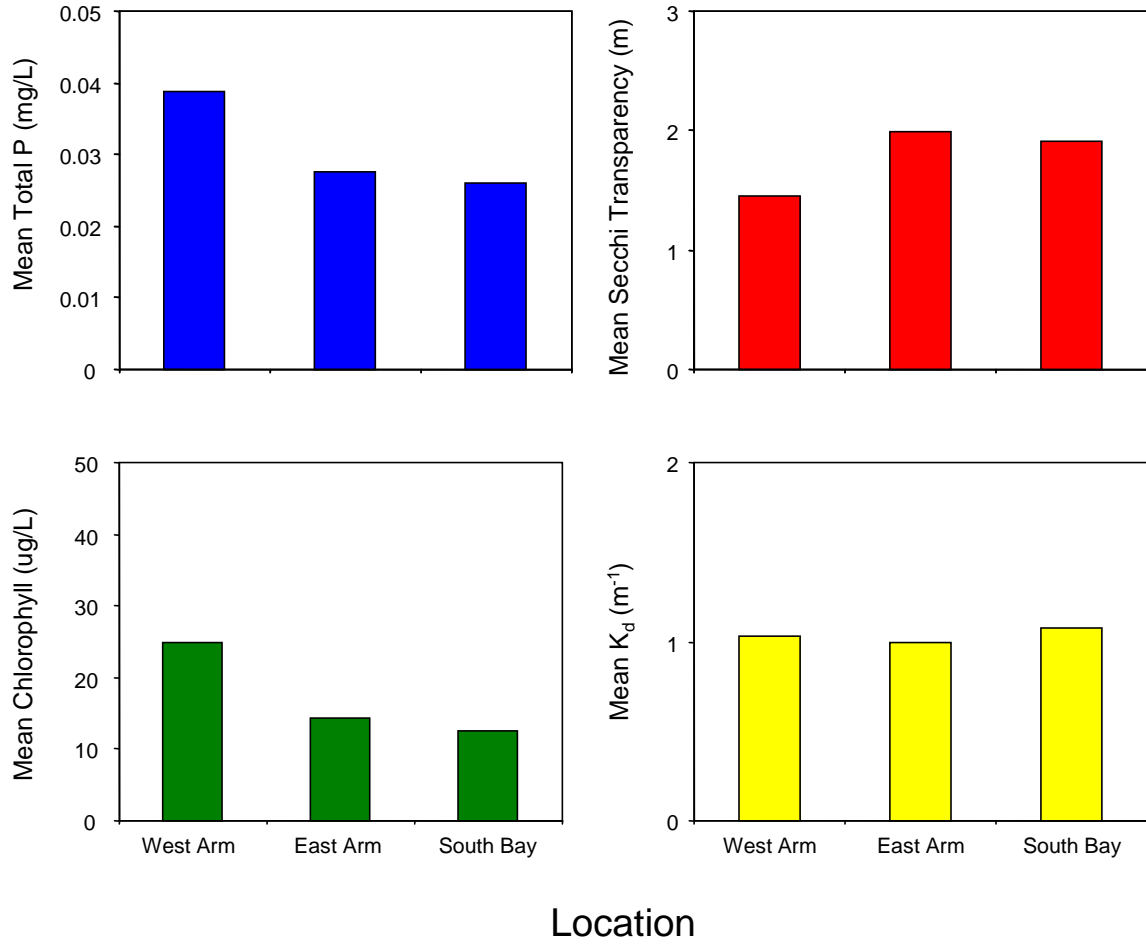


Figure 15. Summer (JUL-SEP) mean total phosphorus (P), chlorophyll, Secchi disk transparency, and photosynthetically active radiation attenuation coefficient (k_d) for the West arm (i.e., stations 10 and 20), East arm (i.e., stations 30 and 40), and South embayment (i.e., station 50) in 2013.

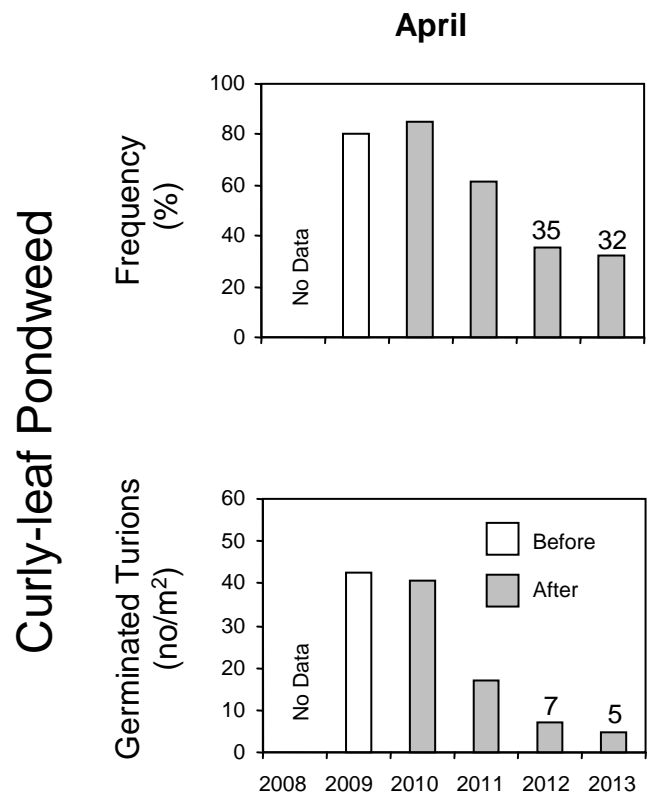


Figure 16. Percent occurrence ($n \sim 140-150$; upper panel) and numbers (lower panel) of germinated curly-leaf pondweed tuions in April of various years. White columns represent means before the start of early spring *Endothall* treatments.

Curly-leaf pondweed

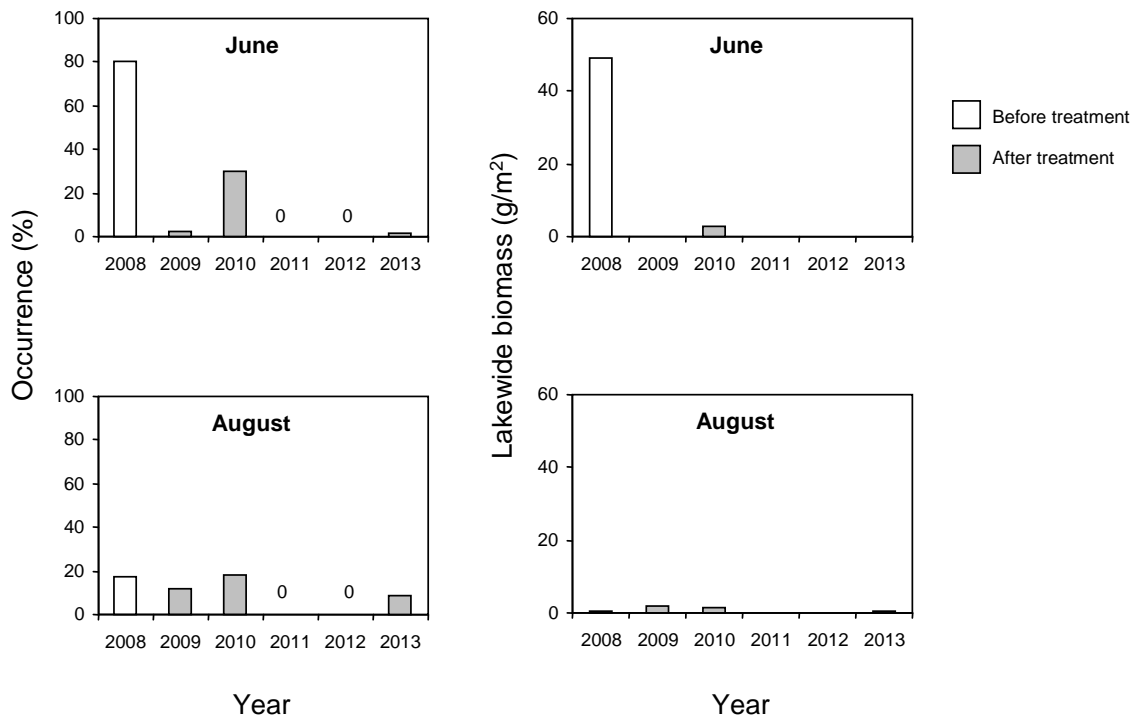


Figure 17. Curly-leaf pondweed lake-wide mean biomass ($n \sim 140-150$) in June and August of various years. White columns represent means before the start of early spring *Endothall* treatments.

Native macrophytes

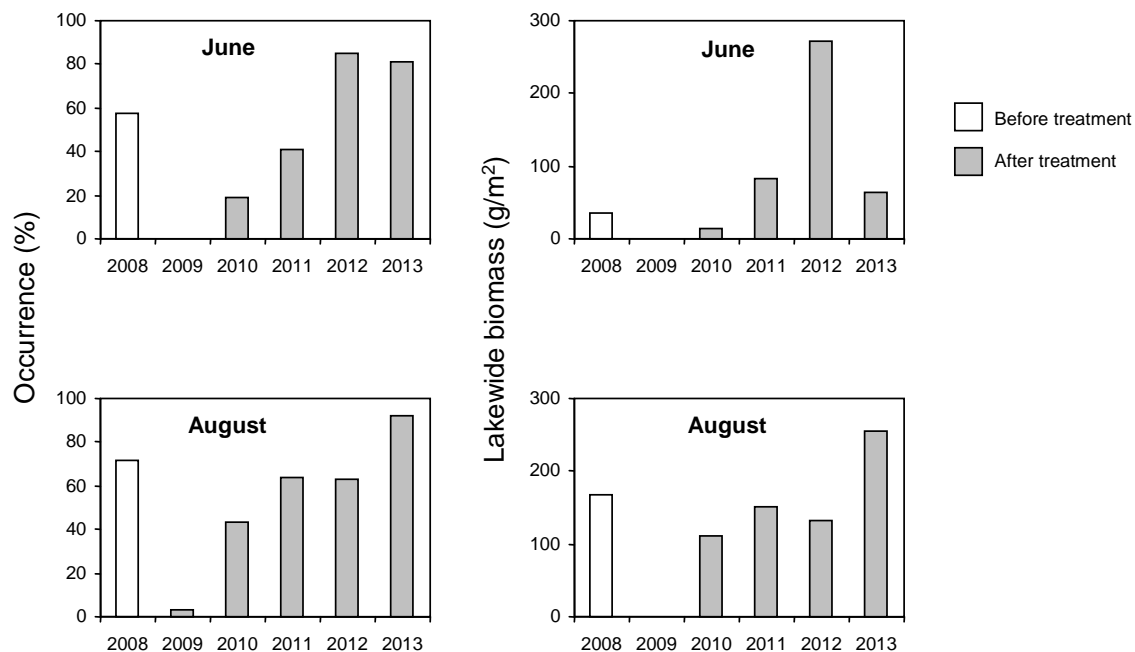


Figure 18. Native submersed macrophyte lake-wide mean biomass ($n \sim 140-150$) in June and August of various years. 2008 was the pretreatment year. The pretreatment native macrophyte community in 2008 was dominated by coontail while elodea has dominated the post-treatment assemblage.

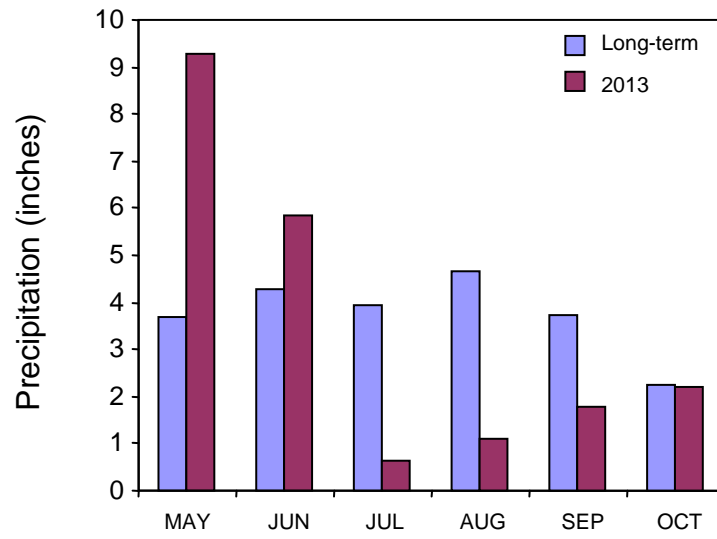


Figure 19. Mean monthly precipitation measured at the Eau Claire Airport.

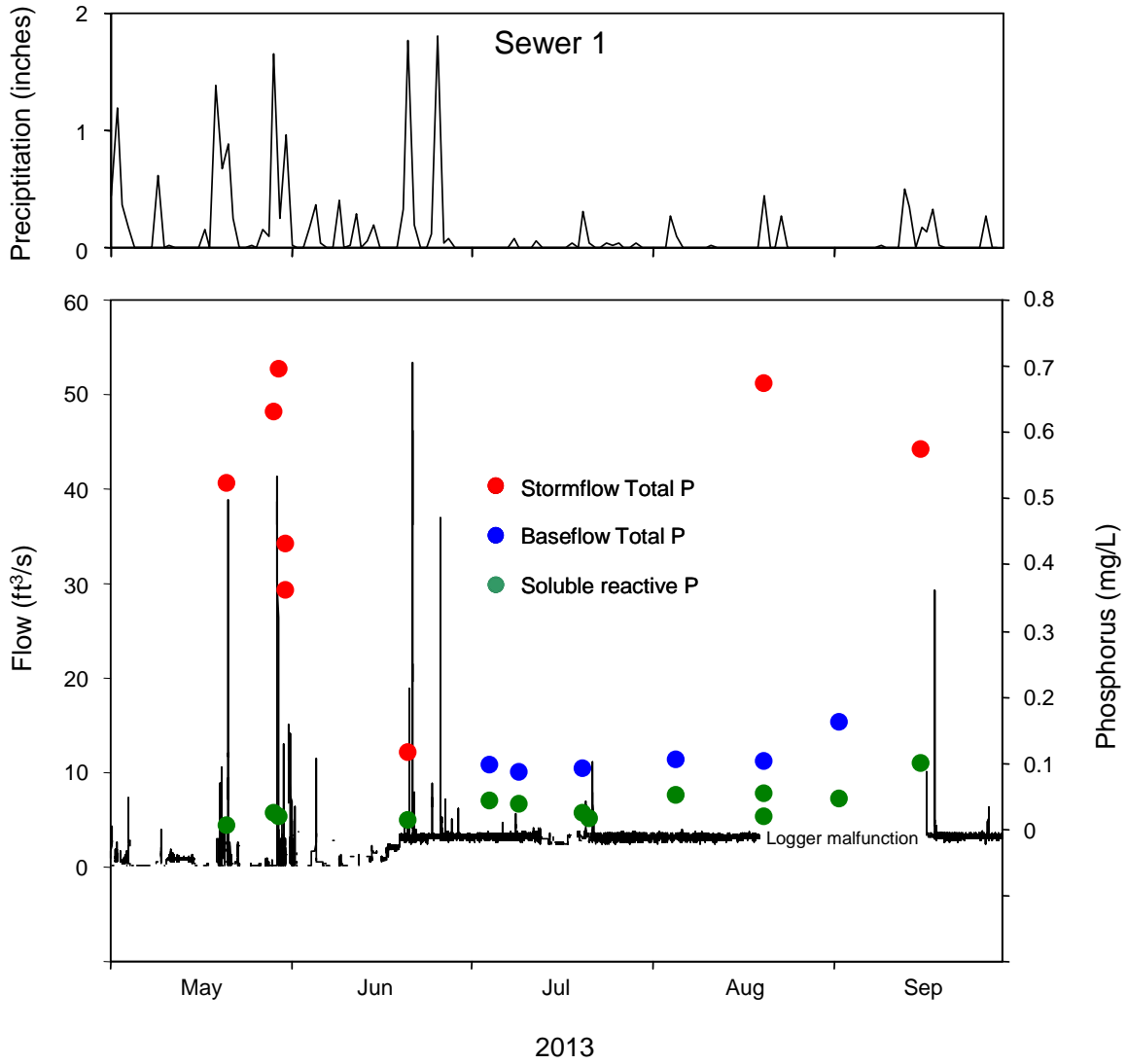


Figure 21. Variations in flow and phosphorus concentrations for storm sewer 1 in 2013.

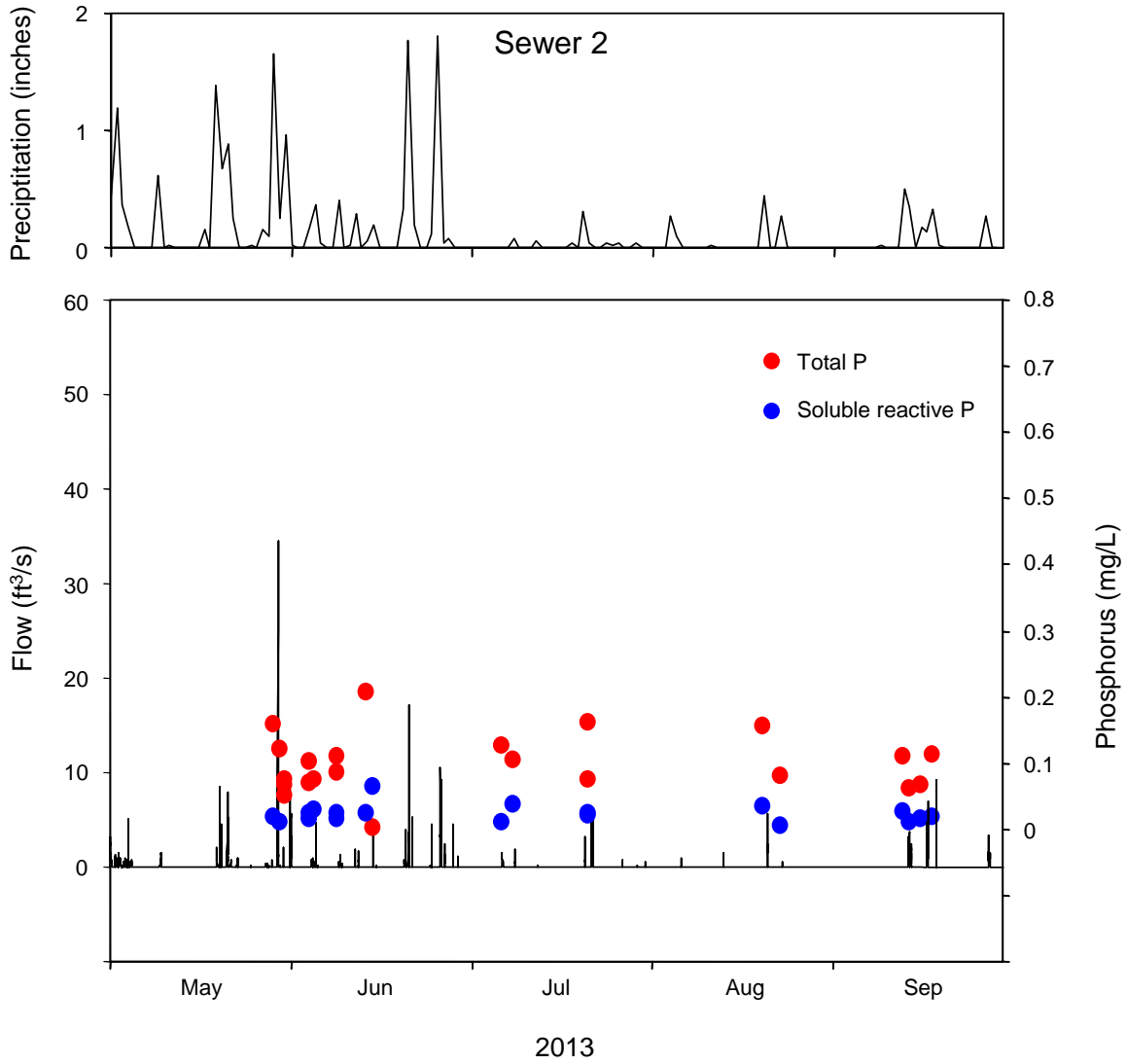


Figure 22. Variations in flow and phosphorus concentrations for storm sewer 2 in 2013.

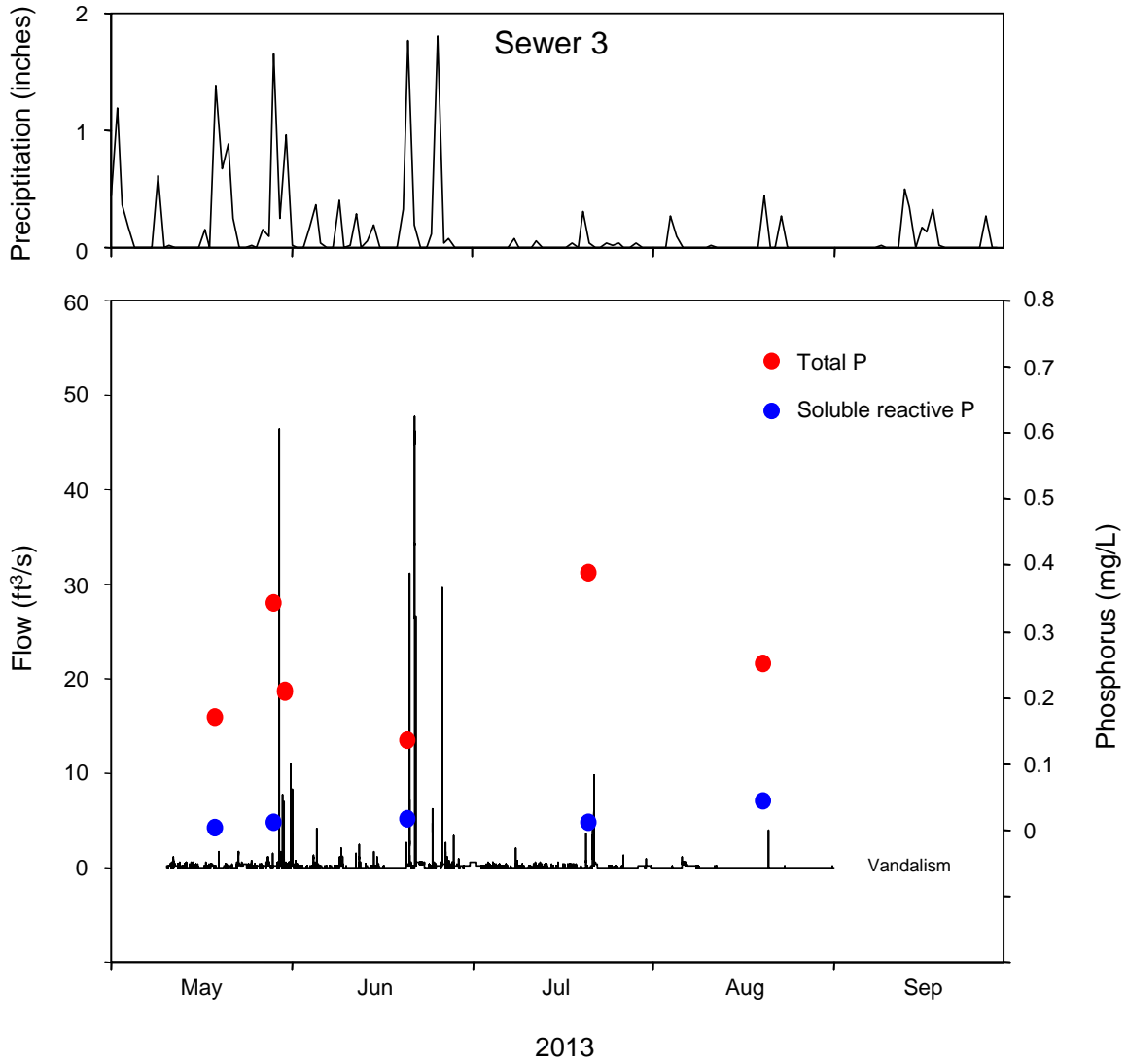


Figure 23. Variations in flow and phosphorus concentrations for storm sewer 3 in 2013.

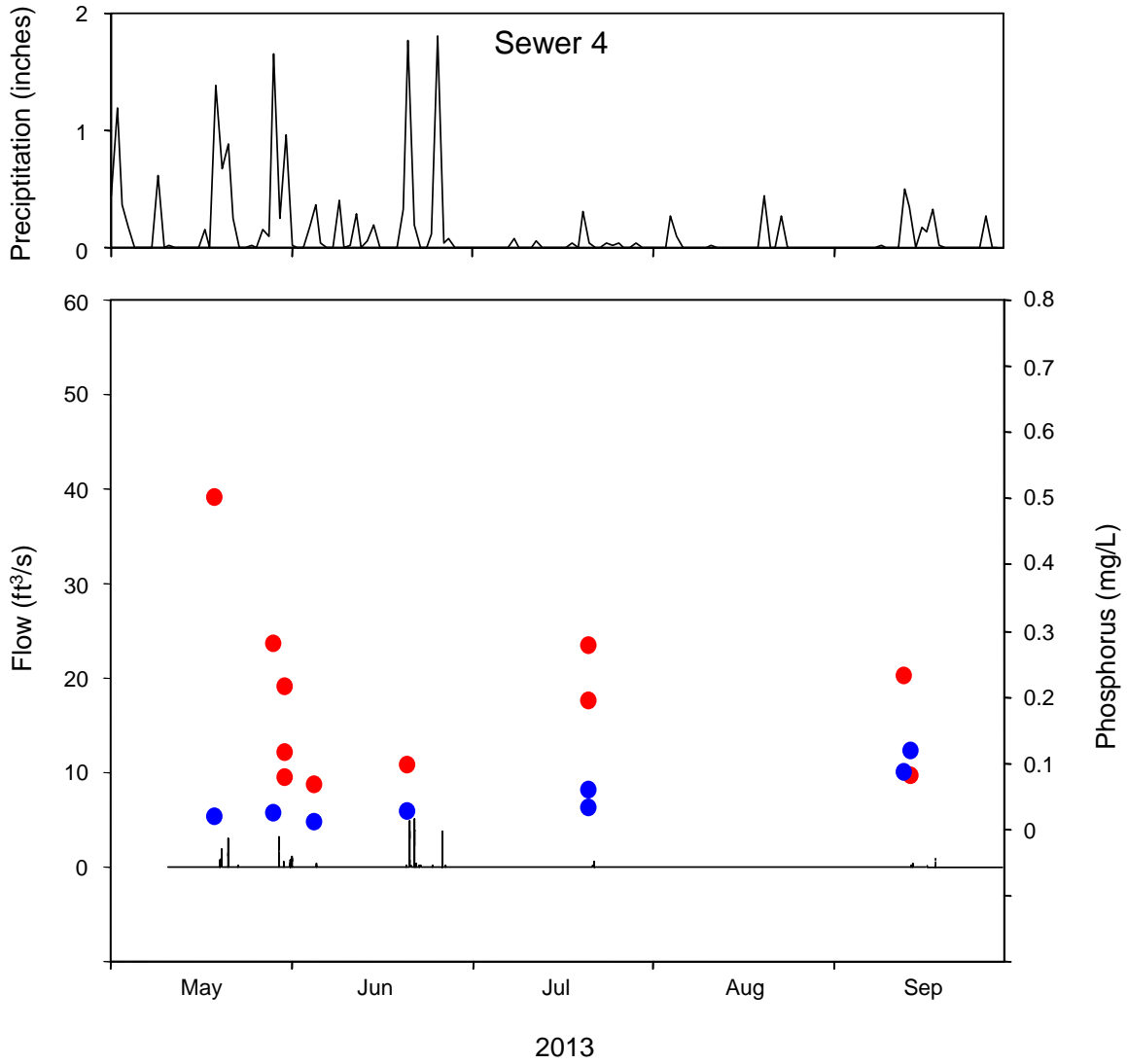


Figure 24. Variations in flow and phosphorus concentrations for storm sewer 4 in 2013.

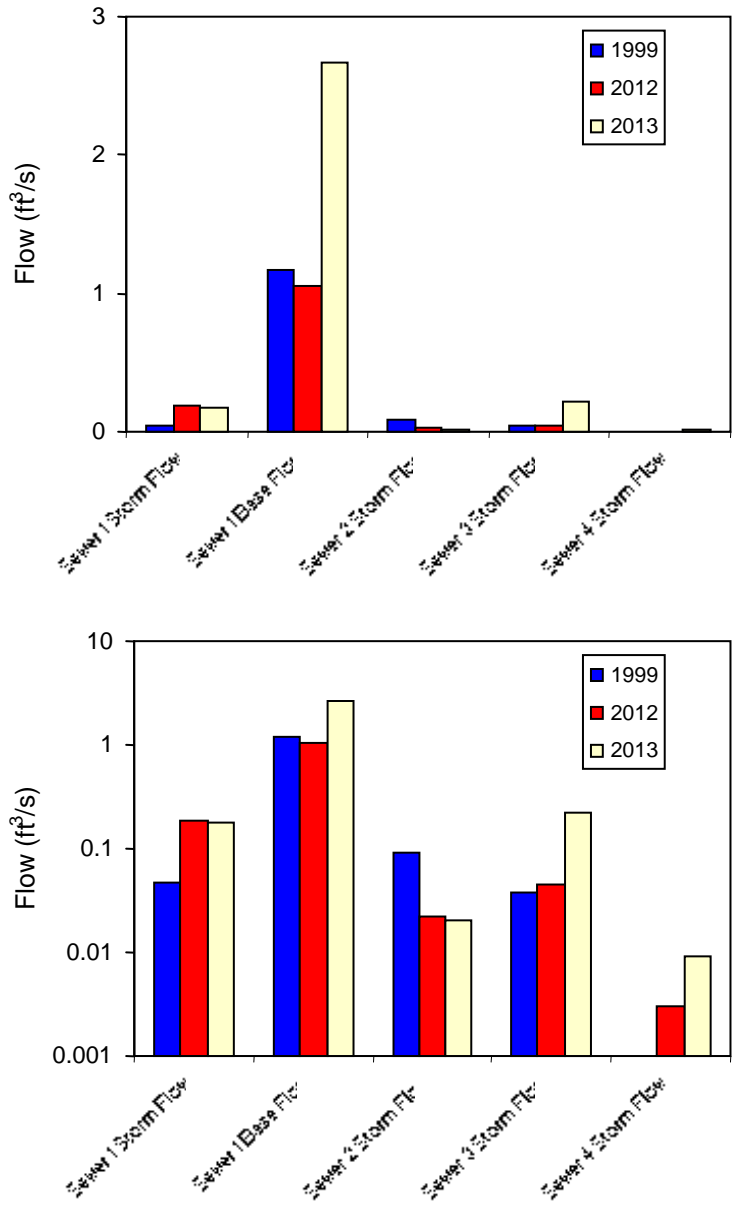


Figure 25. Comparison of mean summer flow at various storm sewers in 1999 and 2012-13. Please note the log scale in the lower panel.

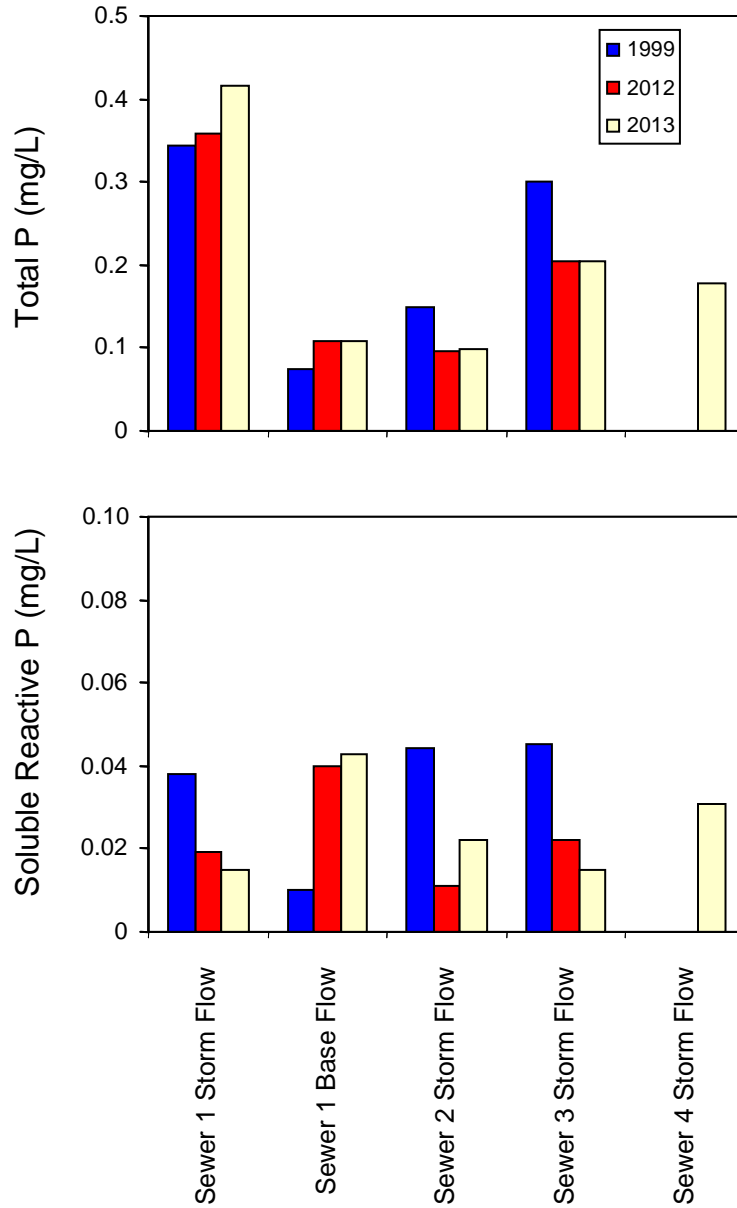


Figure 26. Comparison of flow-weighted total and soluble reactive phosphorus (P) concentrations at various storm sewers in 1999 and 2012-13.

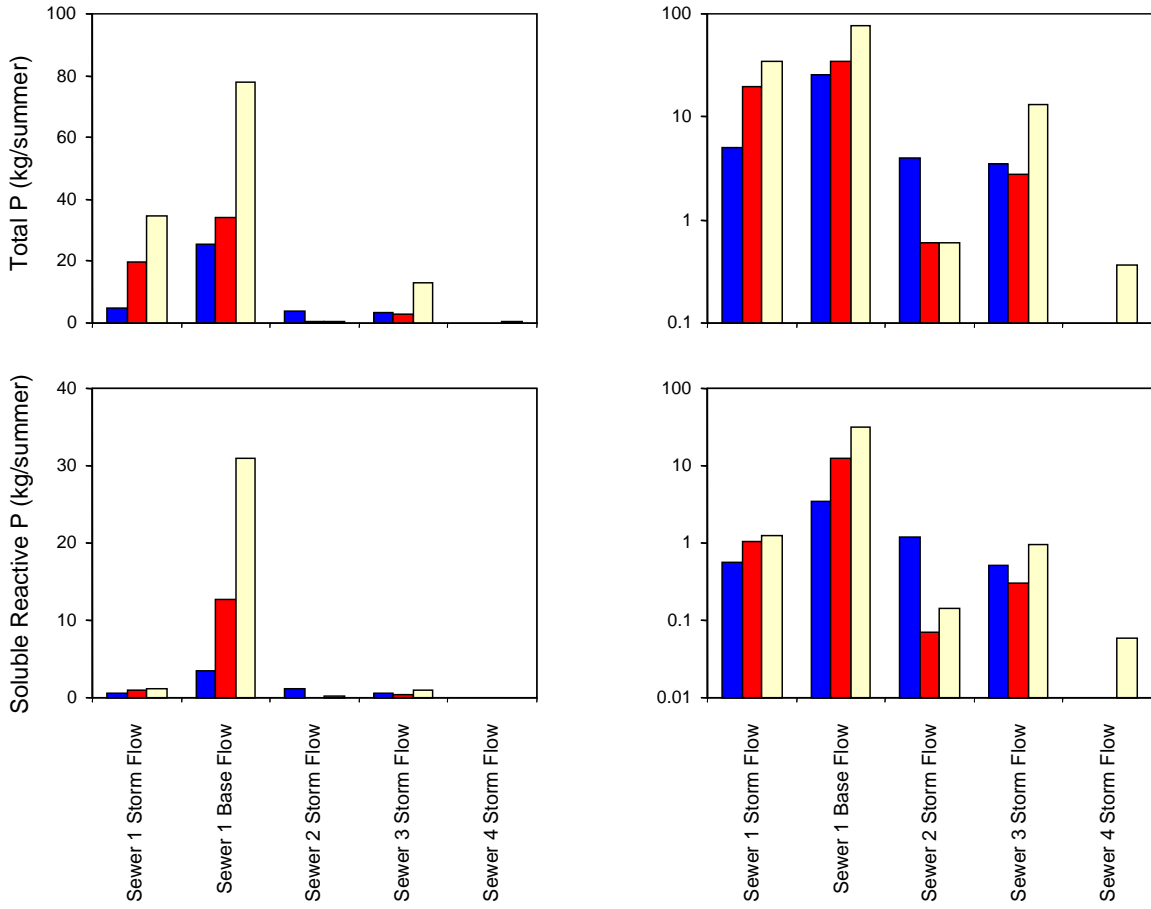


Figure 27. Comparison of total and soluble reactive phosphorus (P) loading at various storm sewers in 1999 and 2012-13.